

**Guy Amit, Khuloud Shukha, Noam Gavriely and Nathan Intrator**

*Am J Physiol Heart Circ Physiol* 296:796-805, 2009. First published Jan 9, 2009;

doi:10.1152/ajpheart.00806.2008

**You might find this additional information useful...**

---

This article cites 25 articles, 6 of which you can access free at:

<http://ajpheart.physiology.org/cgi/content/full/296/3/H796#BIBL>

Updated information and services including high-resolution figures, can be found at:

<http://ajpheart.physiology.org/cgi/content/full/296/3/H796>

Additional material and information about *AJP - Heart and Circulatory Physiology* can be found at:

<http://www.the-aps.org/publications/ajpheart>

---

This information is current as of March 5, 2009 .

## Respiratory modulation of heart sound morphology

Guy Amit,<sup>1</sup> Khuloud Shukha,<sup>2</sup> Noam Gavriely,<sup>2</sup> and Nathan Intrator<sup>1</sup>

<sup>1</sup>School of Computer Science, Tel-Aviv University, Tel-Aviv; and <sup>2</sup>Rappaport Faculty of Medicine, Technion-Israel Institute of Technology, Haifa, Israel

Submitted 2 August 2008; accepted in final form 7 January 2009

**Amit G, Shukha K, Gavriely N, Intrator N.** Respiratory modulation of heart sound morphology. *Am J Physiol Heart Circ Physiol* 296: H796–H805, 2009. First published January 9, 2009; doi:10.1152/ajpheart.00806.2008.—Heart sounds, the acoustic vibrations produced by the mechanical processes of the cardiac cycle, are modulated by respiratory activity. We have used computational techniques of cluster analysis and classification to study the effects of the respiratory phase and the respiratory resistive load on the temporal and morphological properties of the first (S1) and second heart sounds (S2), acquired from 12 healthy volunteers. Heart sounds exhibited strong morphological variability during normal respiration and nearly no variability during apnea. The variability was shown to be periodic, with its estimated period in good agreement with the measured duration of the respiratory cycle. Significant differences were observed between properties of S1 and S2 occurring during inspiration and expiration. S1 was commonly attenuated and slightly delayed during inspiration, whereas S2 was accentuated and its aortic component occurred earlier at late inspiration and early expiration. Typical split morphology was observed for S1 and S2 during inspiration. At high-breathing load, these changes became more prominent and occurred earlier in the respiratory cycle. Unsupervised cluster analysis was able to automatically identify the distinct morphologies associated with different respiratory phases and load. Classification of the respiration phase (inspiration or expiration) from the morphology of S1 achieved an average accuracy of  $87 \pm 7\%$ , and classification of the breathing load was accurate in  $82 \pm 7\%$ . These results suggest that quantitative heart sound analysis can shed light on the relation between respiration and cardiovascular mechanics and may be applied to continuous cardiopulmonary monitoring.

phonocardiography; cardiopulmonary interaction; cluster analysis; classification; noninvasive monitoring

THE MECHANICAL FUNCTION OF the cardiovascular system is governed by a complex interplay between pressure gradients across the chambers of the heart and the blood vessels. The systolic contraction of the ventricles triggers vibrations of the heart walls, valves, and blood. These vibrations propagate through the thoracic cavity and are received on the chest wall as transient low-frequency vibro-acoustic signal, commonly known as the first heart sound, S1. At the end of systole, concomitantly with the abrupt closure of the semilunar valves, the second heart sound, S2, is produced (22). The mechanical cardiac cycle is continuously controlled and regulated by the autonomous nervous system, which induces changes to both rate and intensity of myocardial contraction. In addition, the pulmonary system plays an important part in modulating the cardiovascular mechanical activity by respiratory-induced changes of the pleural pressure, arterial resistance, and venous return (preload) (6, 20). During inspiration, the pressure gra-

dient from the extrathoracic regions to the right atrium increases due to the lowered pleural pressure, causing an increased blood filling of the right ventricle (RV). The increased RV end-diastolic volume (EDV) leads to an increased RV stroke volume (SV) by the Frank-Starling mechanism (7). The distended RV causes the left ventricle (LV) to become less compliant by physical compression (ventricular interdependence) and leftward motion of the interventricular septum, resulting in a reduced LV filling. At the same time, the distending lung and its circulatory volume tend to reduce the pressure gradient and flow from the pulmonary veins to the LV, and the transmural diastolic aortic pressure, which is the LV afterload, increases. These additive effects result in a decrease of LV-SV (25). The opposed process occurs during expiration, in which RV-EDV and RV-SV decrease while LV-EDV and LV-SV increase. The effects of the respiratory cycle and intrathoracic pressure changes on cardiac function are well known clinically in the form of “pulsus paradoxus” as a sign of asthma severity (16) and in assessing the need for fluid transfusion in critically ill patients.

Previous studies have shown effects of hemodynamic changes on characteristics of the heart sounds. The intensity of S1 has been shown to be linearly related to the maximal time derivative of the LV systolic pressure in dogs (23). Spectral features of S1 were correlated with the contractile state of the heart in both dogs (8) and humans (3). The phenomena of split heart sounds, i.e., an audible separation between consecutive components of either S1 or S2 is a well-established example for the relation between heart sounds and the respiratory activity. Physiological split of heart sounds is common in children and young adults. During inspiration, the first component of S1 was found to decrease in intensity, whereas the second component increased, reflecting the different hemodynamic events of the left and right sides of the heart (14, 21). Maximal splitting of S2 was found to occur during inspiration, due to earlier occurrence of the aortic component and a delay in the pulmonary component (21). Respiration has also been shown to modulate the duration of the systolic and diastolic time intervals of the cardiac cycle (29). Quantitative analysis of S2, by spectral and time-frequency techniques, has been suggested as a noninvasive method for estimating pulmonary artery pressure (9). Despite the potential value of phonocardiography-based methods in the study of cardiovascular and cardiopulmonary functions, quantitative analysis of heart sounds is a research field that has been relatively overlooked in recent years, as the focus of cardiovascular diagnosis technologies shifted to imaging techniques, such as echocardiography, nuclear imaging, and computerized tomography. However, the

Address for reprint requests and other correspondence: G. Amit, The School of Computer Science, Faculty of Exact Sciences, Tel-Aviv Univ., P.O.B. 39040, Tel-Aviv 69978, Israel (e-mail: guy.amit@cs.tau.ac.il).

The costs of publication of this article were defrayed in part by the payment of page charges. The article must therefore be hereby marked “advertisement” in accordance with 18 U.S.C. Section 1734 solely to indicate this fact.

vast progress in computation power and analysis algorithms facilitates utilization of modern signal processing and pattern recognition methods in the analysis of heart sounds to extract meaningful physiological information. The purpose of this work was to characterize the morphological changes induced to S1 and S2 by the respiratory activity (Fig. 1). We studied the effects of the respiratory cycle and the respiratory resistive load on the morphologies of S1 and S2, using computational techniques of cluster analysis and classification.

## METHODS

### Experimental Setup

Heart sounds, breathing pressure at the mouth, and a single-lead ECG were simultaneously acquired from 12 healthy volunteers (age  $29 \pm 12$  yr, 8 men). The research protocol was approved by the local ethics committee, and all subjects signed an informed consent before their enrollment in the study. The data-acquisition system consisted of two piezoelectric contact transducers (PPG Sensor model 3, OHK Medical Devices, Haifa, Israel), a breathing pressure transducer (Vali-dyne, Northridge, CA), an ECG recording system (Atlas Researchers, Hod-Hasharon, Israel), a preamplifier (Alpha-Omega, Nazareth, Israel), an analog-to-digital converter (National Instruments, Austin, TX; sampling rate 11,025 samples/s, sample size 16 bits), and a designated signal recording software running on a portable personal computer (Fig. 2). During data recording, the subjects were sitting upright, with the heart sound transducers firmly attached by an elastic strap on the left and right parasternal lines at the fourth intercostal spaces. The data were recorded while the subjects were breathing through a mouthpiece that was side connected to the pressure transducer and serially attached to plastic tubes (internal diameter = 0.5 cm) of varying lengths, used for altering the respiratory resistive loads. Five levels of resistance were used: at level 0, no resistive tube was attached, and at levels 1–4, the lengths of the resistive tubes were 8.5, 22, 66, and 200 cm, respectively. The signals were recorded twice with each resistance level using two breathing protocols: 1) 40 s of normal breathing, and 2) 10 s of normal breathing, followed by 15 s of breath hold and additional 15 s of normal breathing.

### Signal Analysis Framework

Signal analysis (Fig. 3) included the following steps for each subject. A detailed description of the data analysis algorithms, and the

considerations for choosing specific analysis parameters, are given in Ref. 2.

1) Preprocessing and segmentation of S1 and S2 was the first step. Heart sound signals were bandpass filtered in the range of 20–250 Hz and partitioned into cycles by the R-wave of the ECG. S1 was segmented as a 200-ms segment starting 50 ms before the R-wave. For the segmentation of S2, multiple heart sound cycles were averaged, and the two strongest peaks in the energy envelope of the averaged signal were identified. The 200-ms signal fragment, centered at the second energy peak of the average signal, was segmented as S2.

2) The second step was selection of appropriate signal representation in the time or time-frequency domain. S1 signals were represented in the time domain, whereas S2 signals were transformed to a joint time-frequency representation by applying S-transform (28). These signal representations were chosen to obtain an optimal balance between the accuracy of the analysis and the computational efficiency, according to the analysis described in Ref. 2.

3) Hierarchical clustering of S1 and S2 performed on signals from all breathing resistance levels was the third step. Correlation distance was used for estimating the similarity between signal cycles.

4) The fourth step was compact beat representation in the feature space of cluster distances. Each beat was characterized by a vector of its distances from the centers of the significant clusters.

5) The fifth step was analysis of the morphological variability and periodicity of S1 and S2 and their relation to the respiration cycle.

6) The sixth step was prediction of respiration-related measures (respiration phase and resistance) from the morphology of S1 and S2, using classification techniques.

### Cluster Analysis

Cluster analysis was performed on S1 and S2 beats of each subject. Signal similarity measure, used for clustering, was the correlation distance  $D_{sr}$ , defined by:

$$D_{sr} = 1 - \frac{\sum_t (s_t - \bar{s})(r_t - \bar{r})}{\sqrt{\sum_t (s_t - \bar{s})^2} \sqrt{\sum_t (r_t - \bar{r})^2}} \quad (1)$$

where  $t$  is time,  $s_t$  and  $r_t$  are signals of length  $n$ ,  $\bar{s} = \frac{1}{n} \sum_{t=1}^n s_t$  and  $\bar{r} = \frac{1}{n} \sum_{t=1}^n r_t$ .

The maximal number of clusters was set to eight, and only clusters with >5% of the beats were considered significant. Clustering of S1

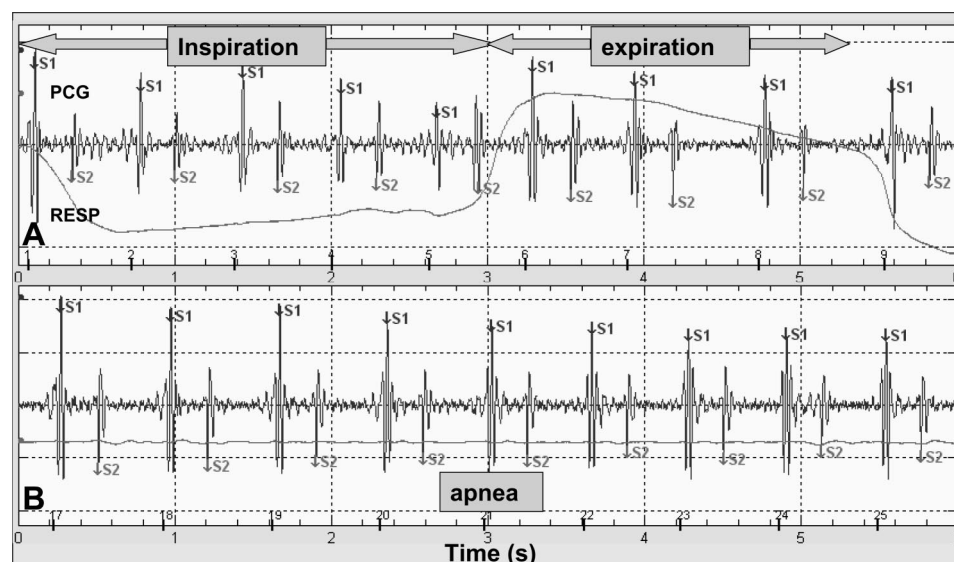


Fig. 1. Morphological variability of heart sounds. A: during a normal respiratory cycle, first (S1) and second (S2) heart sounds exhibit considerable changes in morphology. B: this variability nearly disappears during apnea. RESP, breathing pressure signal; PCG, heart sound signal. Black numbered ticks represent cardiac cycles, according to the R-wave of the ECG.

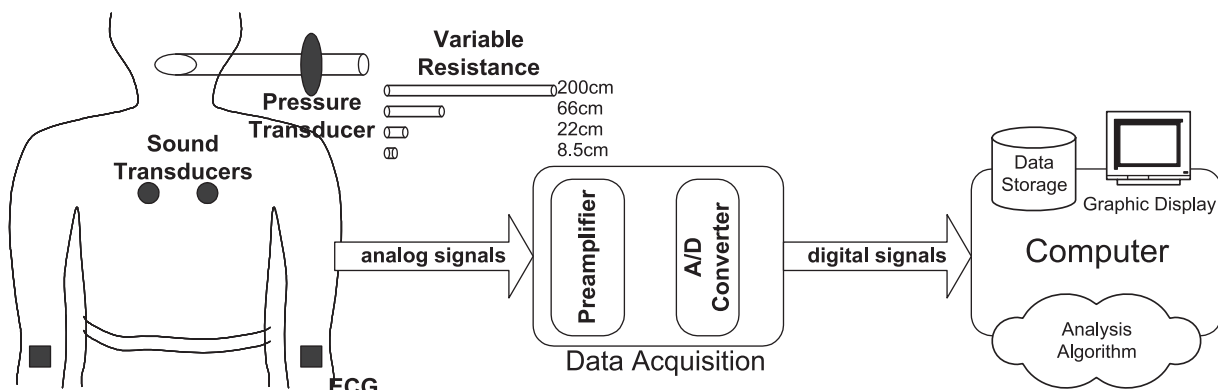


Fig. 2. Experimental setup. Two channels of heart sounds, ECG, and airway-opening pressure are simultaneously acquired, while the subject is breathing against resistive tubes with variable length. The signals are amplified, digitally sampled, and saved for further computational analysis.

was done using raw time domain representation, and clustering of S2 was done on the time-frequency representation of the signals, obtained by S-transform. The center of each cluster was computed as a weighted average of the cluster's elements, in which each element was weighted by its similarity to the cluster's arithmetic mean:

$$\bar{C}_j = \sum_{i \in C_j} \omega_i b_i, \omega_i = 1 - D\left(b_i, \frac{1}{|C_j|} \sum_{i \in C_j} b_i\right) \quad (2)$$

where  $C_j$  is a cluster,  $b_i$  is a beat, and  $D$  is a distance function.

Each beat of S1 and S2 was compactly represented by the vector of its distances from the centers of the  $N$  significant clusters:  $\bar{d}^i = (d_1^i, d_2^i, \dots, d_N^i)$  and  $d_k^i = D(b_i, \bar{C}_k)$ .

*Morphological Clusters and the Respiratory Phase*

Following cluster analysis, the relation between the identified clusters and the respiratory phase was first determined by assessing the morphological variability of S1 and S2 during breathing and apnea. The breathing pressure signal was automatically segmented to identify breathing activity and apnea segments. The median pressure value of the apnea segment in each record was defined as the zero pressure. Pressure values above the zero pressure were considered as "expiration", and pressure values below it were considered "inspiration". The correlation distance between each beat and a template beat, chosen as the average of the largest cluster, was computed. The morphological variability was defined as the standard deviation of this distance, and it was computed for 15-s segments of breathing or apnea. Student's  $t$ -test was used to compare the morphological variability of S1 and S2 during respiration and during apnea across all subjects.

The periodicity of the morphological changes of S1 and S2 was evaluated by applying a robust periodicity detection algorithm (1) on the vectors of cluster center distances. Given  $m$  beats, the vector of their distances from the center of cluster  $k$  can be written as  $\bar{d}_k = (d_k^1, d_k^2, \dots, d_k^m)$ .  $\bar{d}_k$  is nonuniformly sampled, due to the beat-to-beat heart rate variability, and it may contain outlier beats, resulting from noise interferences. The periodicity analysis is based on a robust power spectral estimate, followed by Fisher's  $g$ -test (12), which computes the  $P$  value of the null hypothesis that the time series is a Gaussian noise against the alternative hypothesis that the signal contains an added deterministic periodic component of unspecified frequency. Multiple test corrections for the  $P$  value's cutoff were done using the false discovery rate (FDR) method (4). The cluster center that provided the smallest  $P$  value was selected as a template, and the identified period was compared with the average period of the breathing pressure signal.

To test whether there is a morphological separation between beats that occurs during different phases of the respiratory cycle, each respiration cycle was mapped into the polar phase range 0–360°, where 90° is the peak of inspiration (maximal negative pressure), and 270° is the peak of expiration (maximal positive pressure). Each beat of S1 and S2 was associated with the corresponding value of the instantaneous respiratory phase (0–360°) and with the distance from the chosen cluster center. A two-tailed Student's  $t$ -test was used to compare the distance value distribution of the beats occurring during inspiration (respiration phase value in the range 45–135°) and the beats occurring during expiration (respiration phase value in the range 225–315°). Significant  $P$  value cutoff was determined by the FDR method.

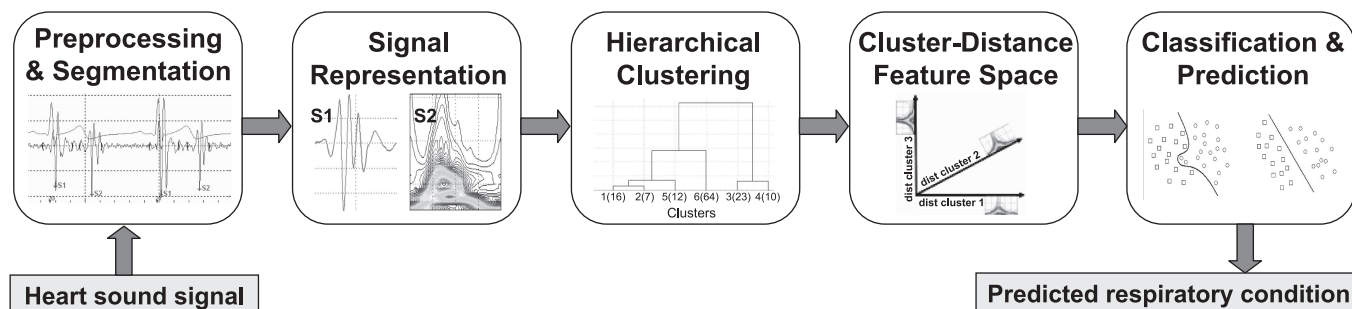


Fig. 3. Signal analysis framework. Input heart sound and ECG signals are preprocessed and segmented to extract S1 and S2 from each cardiac cycle. Signals are then represented by time or time-frequency representation and clustered according to their morphologies. Distances from the centers of the clusters are used as a compact feature space of the data, and classification algorithms are applied in this space to predict the respiratory phase and resistance level.

The ability of the computational analysis framework to predict the respiratory phase from the morphology of S1 or S2 was evaluated separately for each subject. A K-nearest-neighbor classifier was trained on one-half of the beats (using  $K = 5$ ), and its performance was tested on the rest of the beats, by evaluating the accuracy of classifying beats into the correct half of the respiratory cycle.

#### Morphological Clusters and the Respiratory Resistance

The morphological changes of the heart sounds, induced by the changes in the respiratory resistive load, were examined by evaluating the performance of a classifier in predicting the level of respiratory resistive load from the signal's morphology. For this classification task, each beat was labeled by the level of breathing resistance used while it was acquired (R0–R4). For each subject, a K-nearest-neighbor classifier ( $K = 5$ ) was trained on one-half of the beats, and the accuracy of resistance classification was evaluated on the other half by computing  $CC_m$ , the percentage of test beats classified within range  $m$  of their actual resistance level.

$$CC_m = \frac{|\{i \in \text{Test} \mid |\tilde{l}_i - l_i| \leq m\}|}{|\text{Test}|} \quad (3)$$

where  $l_i$  and  $\tilde{l}_i$  are the actual and the estimated respiratory resistance levels of beat  $i$ , respectively. Since the different resistance levels represent a continuum of physiological changes, rather than dichotomic classes,  $CC_1$  was used as a measure of the classification performance. In addition to measuring the correct classification rate per beat, the ability to correctly classify the resistance level of the entire recording, based on the classification of the majority of beats, was evaluated.

## RESULTS

Analyzed data of all 12 subjects included 120 recordings of a total of 6,373 heartbeats acquired during normal respiration (mean  $\pm$  SD:  $531 \pm 74$ ) and additional 6,275 heartbeats acquired during alternations between respiration and apnea (mean  $\pm$  SD:  $523 \pm 73$ ). Cluster analysis, applied to the normal respiration recordings, identified, on average,  $5.5 \pm 1.6$

significant clusters of S1 and  $6.5 \pm 0.9$  significant clusters of S2, containing 96% of the recorded beats.

#### Morphological Variability of Heart Sounds

During normal respiration, both S1 and S2 exhibited marked beat-to-beat variability, which nearly disappeared during apnea (Fig. 4A). The heart sound variability was periodic and apparently synchronized with the respiratory cycle. The average morphological variability of S1, defined as the standard deviation of the correlation distances from a template beat, was  $0.1 \pm 0.07$  during respiration and  $0.03 \pm 0.03$  during apnea (Fig. 4B). For S2, the average variability was  $0.14 \pm 0.09$  during respiration and  $0.06 \pm 0.07$  during apnea (Fig. 4C). Both paired and unpaired  $t$ -tests showed that the variability of S1 and S2 during respiration was significantly higher than during apnea ( $P < 10^{-9}$  for all tests).

Cluster analysis identified distinct morphologies of S1 and S2 in all of the subjects. Although the heart sound morphology varied considerably between subjects, some general observations could be made about the intrasubject morphological changes. A typical example of S1 clusters is shown in Fig. 5A. The major component of S1, prominent in all clusters, is a large high-frequency vibration, which reaches its energy peaks  $\sim 40$  ms after the R-wave of the ECG (90 ms from the beginning of S1 segment). While in the average of the nonclustered signals, the segment that follows the main component is noninformative due to the high interbeat variability, in some of the clusters (for example, the inspiratory clusters 1, 2, 5, and 6), a peak of a secondary low-frequency component is clearly recognized 50–60 ms after the peak of the main component. This “split” of S1 is absent from other significant clusters (for example, expiratory clusters 3, 4, and 8). A similar split could be observed in the clustered time-frequency representation of S2, shown in Fig. 6. In this example, the clustering procedure identified a gradual emergence of a small low-frequency com-

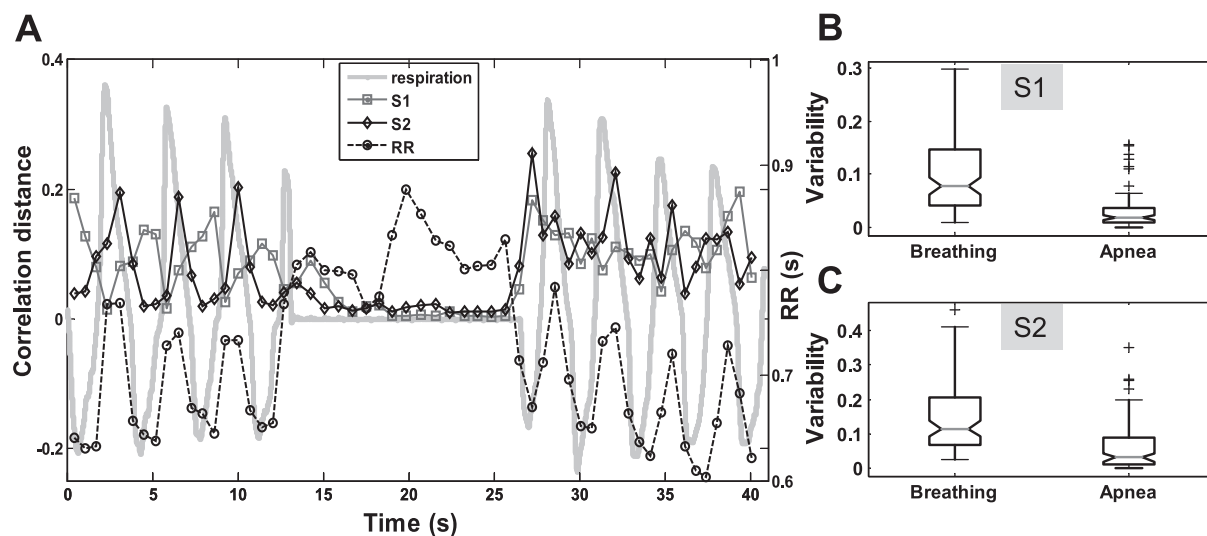
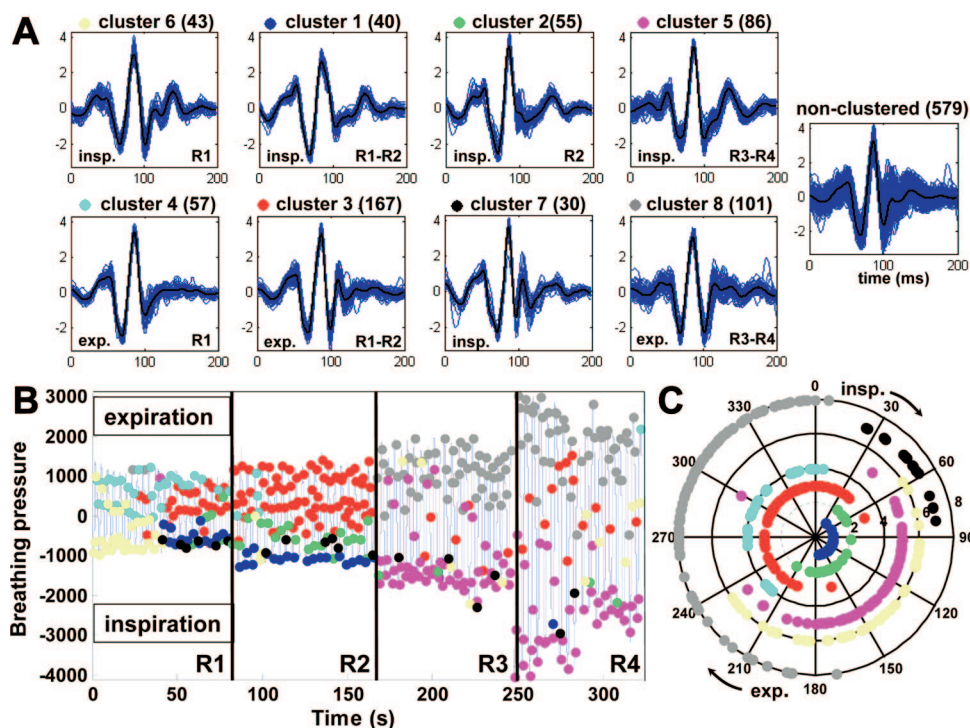


Fig. 4. Respiration-induced variability. A: respiration pressure signal from a single recording (in arbitrary units) with beat variability of S1, S2, and heart rhythm (RR interval) during normal respiration against high resistance and during apnea. Heart sound variability is represented by the correlation distance between each beat and a fixed template. Both S1 and S2 exhibit periodic morphological changes during respiration that diminish during apnea. The standard deviation of the correlation distance during respiration in all subjects is significantly higher than during apnea ( $P < 10^{-9}$ ) for both S1 (B) and S2 (C). The box plots display the median, lower and upper quartiles, data extent, and outliers.

Fig. 5. A: clustering results of 579 beats of S1 acquired from a single subject (NM2) while breathing against variable resistance levels R1–R4. For each of the 8 clusters, the number of beats in the cluster is indicated, and the beats are plotted with the cluster’s average. The morphological variability of the clustered signals is significantly lower than the variability of the nonclustered data, in which subtle changes of the morphology are smeared. The relation between the morphological clusters and the respiratory activity is revealed by plotting the color-coded temporal location of the clustered beats along with the breathing pressure (B) and by a polar display of the phase in the respiratory cycle associated with each beat (C). A marked separation exists between inspiratory and expiratory clusters and between low- and high-breathing resistance levels. Note the secondary peak of energy at ~140 ms in the inspiratory clusters’ morphology (yellow, blue, green, and magenta clusters) that is missing in the expiratory clusters (cyan, red, gray).



ponent, peaking 75 ms after the larger, high-frequency major component. This second component is blurred in the nonclustered average of the S2 segments.

*Periodicity of Heart Sound Morphological Variability*

Statistical analysis of the periodicity of the aforementioned morphological changes was performed on 96 recordings

from all 12 subjects, breathing against four levels of breathing resistance (2 recordings per resistance level per subject). Thresholds for significant *P* values were determined by setting the FDR to 0.01. For S1 signals, a significant periodic component (corrected *P* < 0.007) was identified in 81 of the recordings (84%). For eight subjects, periodicity was identified in all recordings, while for all

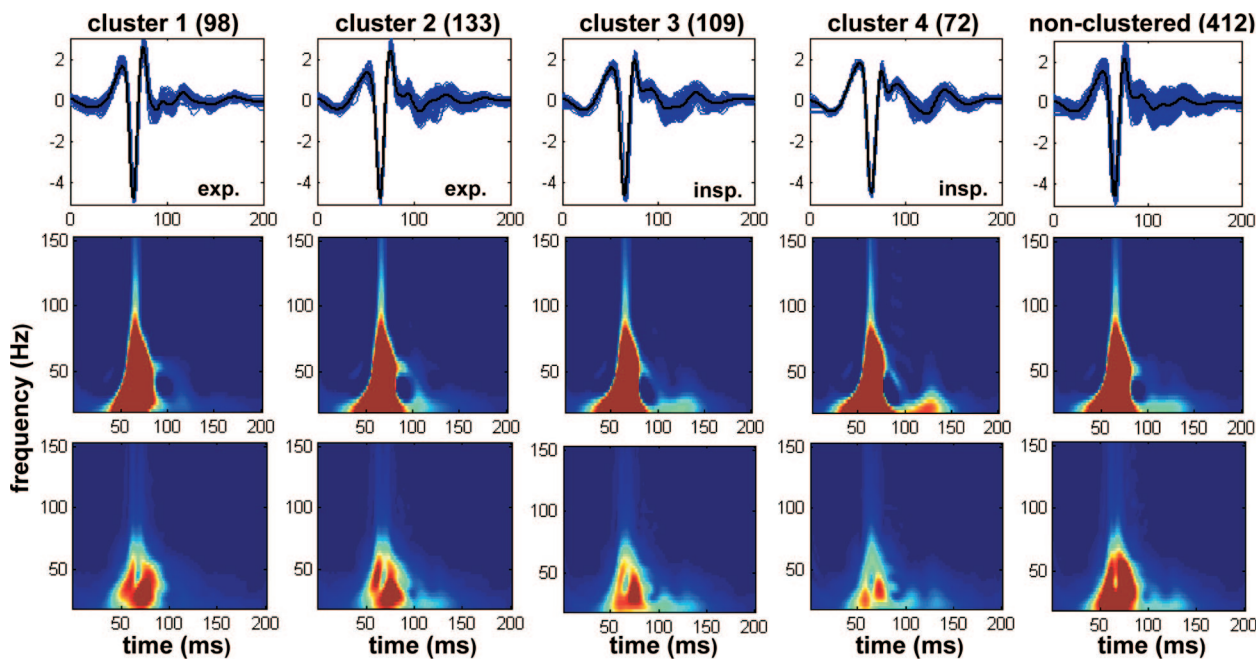


Fig. 6. Clustering results of 412 beats of S2 from a single subject (ST1). For each of the 4 significant clusters, as well as for the nonclustered data, the number of beats in the cluster is indicated, and the beats are plotted with the cluster’s average (top). The centers of the clusters, viewed by a time-frequency representation (middle), emphasizes the emergence of a low-frequency late component in clusters 3 and 4. The standard deviation of the time-frequency representations (bottom) demonstrates the larger morphological variability of the nonclustered data.

subjects periodicity was identified in at least two different recordings. The measured period of S1 morphological changes was in high correlation ( $R = 0.96$ ) and good agreement (mean difference  $0.02 \pm 0.3$  s) with the average period of the respiration cycle, measured from the breathing pressure signal (Fig. 7). For S2 signals, significant periodicity (corrected  $P < 0.006$ ) was identified in 63 of the recordings (66%). All subjects had at least two recordings with periodic S2 morphology, with a good correlation and agreement ( $R = 0.87$ , mean difference  $0.08 \pm 0.5$  s) between the measured period and the actual respiratory period.

#### Modulation of Heart Sounds by the Respiratory Phase

The morphological difference between inspiratory and expiratory beats of S1, measured by comparing the distributions of the distances from a template beat, was found to be statistically significant (corrected  $P < 0.008$ ) in 83 of the recordings (86%), indicating that at least some of the variability in the signal's morphology is related to the respiratory phase. To visualize the effects of the respiratory phase on the heart sounds, S1 and S2 beats were sorted by their time of occurrence in the respiratory cycle ( $0$ – $360^\circ$ ) and plotted as two-dimensional color-coded maps (Fig. 8). The following observations were made regarding the variability of the heart sounds during the respiratory cycle.

**Energy content of S1.** In 11 of 12 subjects, there was a statistically significant difference ( $P < 0.001$ ) between the energy content of S1 beats occurring in proximity to peak inspiration (phase range  $45$ – $135^\circ$ ) and beats occurring in proximity to peak expiration (phase range  $225$ – $315^\circ$ ). In nine of these subjects, S1 was attenuated during inspiration (phase  $0$ – $180^\circ$ ) and accentuated during expiration (phase  $180$ – $360^\circ$ ). In the remaining two subjects, the opposite relation was observed.

**Timing of S1.** S1 was slightly delayed during inspiration in all 12 subjects. The temporal delay from the R-wave of the ECG to the peak energy point of S1 was  $4$ – $20$  ms longer in inspiratory beats compared with expiratory beats (mean  $12 \pm 6$  ms). This difference was statistically significant ( $P < 10^{-6}$ ) in 10 of the subjects.

**Split of S1.** In six subjects, a low-frequency second component was clearly identified in S1 signals occurring during inspiration or early expiration. The peak of this component was typically  $50$ – $60$  ms after the peak of the major, high-frequency component.

**Energy content of S2.** In all of the subjects, the energy content of S2 was significantly higher ( $P < 0.001$ ) during late inspiration and early expiration (phase range  $135$ – $225^\circ$ ), compared with late expiration and early inspiration (phase range  $315$ – $45^\circ$ ).

**Timing of S2.** S2 occurred earlier during late inspiration and early expiration in 11 of the subjects. The peak energy of S2 during this respiratory phase occurred  $6$ – $28$  ms earlier, compared with late expiration and early inspiration beats ( $P < 0.001$ ).

**Split of S2.** The changes in the timing of S2 during late inspiration and early expiration was typically due to the earlier occurrence of the first, aortic component of S2, while the second, pulmonary component did not change or was slightly delayed, producing a noticeable split-S2 morphology in nine of the subjects.

The ability of the cluster analysis framework to automatically identify the relations between the morphology of S1 and the respiratory phase is demonstrated in Fig. 5B. There is a marked separation between clusters on the breathing pressure axis: some clusters (e.g., clusters 1, 5, and 6) contain beats that occur in proximity to the peak of inspiration (maximal negative pressure), while other clusters (e.g., clusters 3, 4, and 8) are dominated by beats that occur during expiration (positive pressure). This separation is even more apparent in Fig. 5C, showing the distribution of each cluster along the phase of the respiratory cycle. Beats of either S1 or S2 that are associated with inspiration are characterized by the split morphology, wherein a second low-frequency component follows the major higher frequency component, as described in the previous section. The clusters without this low-frequency component are typically associated with the expiratory or transition phases of the respiration cycle.

The accuracy of the respiratory-phase classification from the heart sound morphology of all subjects is given in Table 1. The cluster-distance representation of S1 morphologies provided

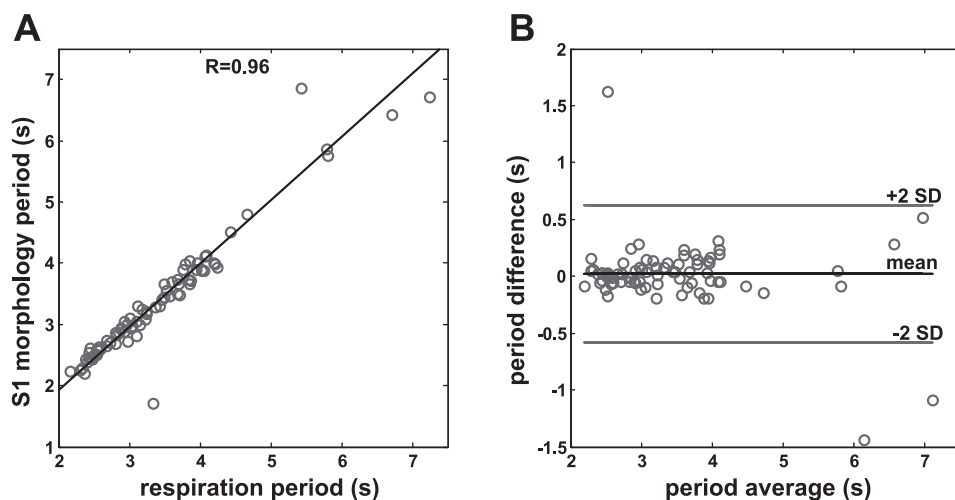


Fig. 7. A linear regression plot (A) and a Bland-Altman plot (B) showing the strong correlation and the good statistical agreement between the period of the morphological changes of S1 and the actual respiration period.

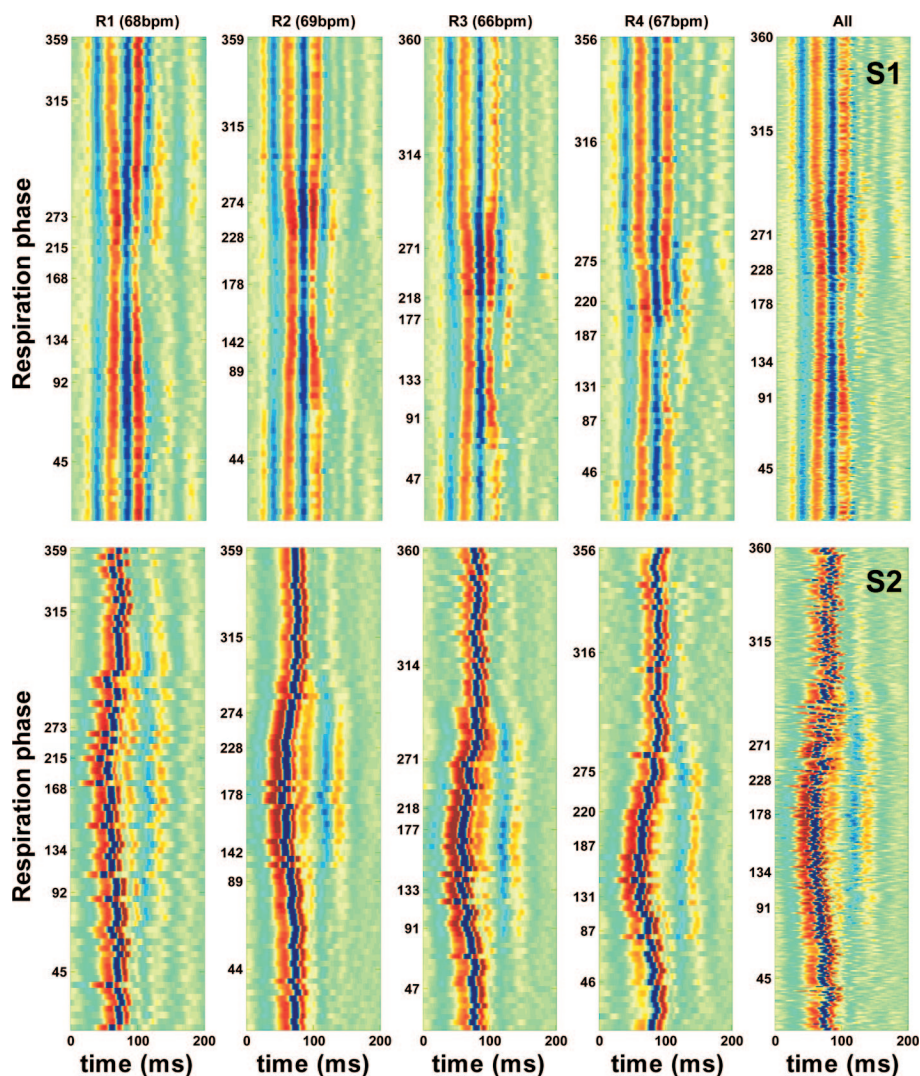


Fig. 8. Morphological and temporal changes of S1 (top) and S2 (bottom), induced by the respiratory phase and load (subject ST1). S1 and S2 beats of each separate resistance level (R1–R4) and of the entire recording set (All) were sorted by the phase of their occurrence in the respiratory cycle (0–360° with inspiration occurring around 90° and expiration around 270°) and plotted as color-coded maps (red indicating positive deflection of the signal). Note that the respiration phase axis in each plot is slightly different, due to the arbitrary occurrence times of heartbeats during respiration. S1 is delayed and attenuated during late inspiration. S2 occurs earlier and exhibits split morphology during late inspiration and early expiration. As the breathing load (resistance) is higher, these changes become more prominent and occur earlier in the respiration cycle. bpm, Beats/min.

good separation between beats associated with different halves of the respiratory cycle. Best accuracy was achieved for partitioning the respiratory cycle at the points of phase 30° and 210°, allowing small error tolerance during transitions between inspiration and expiration. The accuracy of the phase classification varied between subjects, from 75 to 97% (average  $87 \pm 7\%$ ). Phase classification using the morphology of S2 was much less accurate than S1, with an average correct classification of  $69 \pm 8\%$ , indicating that the morphological changes in S2 during respiration are less predictable than the changes in S1.

#### Modulation of Heart Sounds by the Respiratory Resistive Load

In addition to the cyclic morphological changes induced to the heart sounds by the respiratory phase, there are also changes induced by the extent of the respiratory resistive load (Fig. 8). The changes in the temporal location of S1 and S2 are more prominent when the breathing load is higher. The delay of S1 during inspiration becomes longer and the delay of S2 during late inspiration/early expiration becomes shorter in high-breathing resistances, compared with low-breathing resis-

tances. In some of the subjects, the magnitude of the changes in the energy and morphology of the heart sounds was also related to the level of breathing resistance. Furthermore, the resistance level affected the occurrence time of the aforementioned changes in the respiratory cycle: as the breathing load was higher, the respiration-induced changes of the heart sounds occurred earlier in inspiration. This was observed in 10 of the subjects for temporal, morphological, or energy-related changes of S1 and S2.

Cluster analysis was able to recognize resistance-induced changes, as shown in Fig. 5B: while breathing against high resistance levels (R3 and R4), distinct clusters of S1 were identified for both inspiratory and expiratory phases. The ability of the clustering and classification framework to correctly identify the breathing resistance from the beat's morphology was quantified by the classification results given in Table 1. The accuracy of resistance classification with a maximal one-level error ( $CC_1$ ) varied from 65 to 90% (mean  $82 \pm 7\%$ ) using S1, and from 57 to 90% (mean  $73 \pm 11\%$ ) using S2. With S1-based classification, 51% of the beats in the entire test set were classified to their exact resistance level ( $CC_0$ ), and 93% were classified with a maximal two-level error ( $CC_2$ ),

Table 1. Results of cluster analysis and classification of the respiratory phase and resistance from the morphology of S1 and S2

Subject ID	Age, yr	Sex	Beats, no.	S1			S2		
				Clusters, no.	Phase-CC, %	Resist-CC <sub>1</sub> , %	Clusters, no.	Phase-CC, %	Resist-CC <sub>1</sub> , %
GA1	31	M	528	5	92	74	7	64	57
ND1	21	F	652	4	96	81	6	71	76
NM1	24	M	534	8	83	85	6	65	88
NG1	53	M	479	5	94	81	8	79	61
NM2	25	M	579	5	93	87	6	72	77
ND2	19	F	544	4	75	65	5	57	75
NM3	20	F	562	7	97	74	6	65	63
OG1	24	M	631	4	84	85	6	79	79
ST1	22	M	442	7	89	84	7	82	90
ZM1	20	F	557	4	83	83	6	60	63
RS1	54	M	455	8	81	90	7	59	79
SS1	37	M	410	5	79	89	8	72	71
Mean	29.2		531.1	5.5	87.1	81.6	6.5	68.8	73.3
SD	12.5		73.7	1.6	7.2	7.3	0.9	8.4	10.6

S1, first heart sound; S2, second heart sound; M, male; F, female; clusters, number of significant clusters, containing at least 5% of the beats; CC, correct classification of respiratory phase is the percentage of beats correctly classified as "expiration" or "inspiration"; CC<sub>1</sub>, correct classification of respiratory resistance is the percentage of beats classified within one level error of their actual resistive load.

indicating that there is a good separation between low-resistance and high-resistance beats. Since, for practical applications, resistance classification may be needed for a series of beats rather than for a single beat, the classification performance per test recording was also evaluated. Automatic classification of the resistance level of the entire recording, using the majority classification of the recording's beats, was exact (CC<sub>0</sub>) in 45 of the 60 test recordings (75%), and correct with maximal one-level error (CC<sub>1</sub>) in 55 of the recordings (92%).

## DISCUSSION

Heart sounds are produced by the vibrations of the cardiovascular system, composed of the blood, heart walls, and valves. The vibrations are triggered by the acceleration and deceleration of blood due to the abrupt mechanical events of the cardiac cycle (18, 22). The mechanical events producing the components of the S1 are the onset of ventricular contraction, the closure of the atrioventricular valves, and the onset of blood ejection through the semilunar valves. The closure of the semilunar valves at the end of systole is the main mechanical event leading to the S2. The complex interplay between pressure gradients in the atria, passive and active muscle tension of the ventricles, and arterial pressure and distensibility affect the timing, magnitude, and morphology of the produced heart sounds. The amplitude of S1 has been shown to be related to the degree of separation of the mitral valve leaflets, determined by the relative timing of the left atrial and ventricular systole. LV contractility was also shown to be an independent factor determining the amplitude of S1 (23, 27). The amplitude of the aortic component of S2 has been shown to be closely related to the peak rate of development of the aortic-to-LV differential pressure gradient (17). The dyssynchrony between the dynamics of the left and right sides of the heart has well-established effects on widening the delay between the sound components, thus producing a split morphology of either S1 or S2 (14, 21). The cyclic respiratory activity modulates the mechanical function of the left and right heart through changes in the pleural pressure (Fig. 9) and pulmonary blood flow. The lowered

pleural pressure during inspiration causes enhanced venous return to the right atrium and increased preload and SV of the RV. The preload and SV of the LV are decreased due to ventricular interdependence and increased afterload (7, 25). The LV contracts with a decreased force, against a higher arterial resistance, and S1 is attenuated. The increased difference between aortic and LV pressure causes S2 to be accentuated. In addition, the aortic component of S2 occurs earlier, while the pulmonary component is delayed as the RV pressure is high. These temporal changes result in a wider split of S2.

The results presented in this paper confirm this physiological model using modern computational analysis. The clustering of heart sounds, along with the compact representation of the signal morphology in the feature space of cluster distances, enabled us to quantitatively analyze the complex relationship between heart sounds and respiratory activity. Both S1 and S2 exhibited strong morphological variability during respiration, and nearly no variability during apnea. The morphological variability of heart sounds was found to be periodic, and the estimated period was in good agreement with the measured duration of the respiration cycle. This apparent relation between the respiration phase and the characteristics of the heart sounds was confirmed by identifying statistically significant differences in the template-based distance, the energy content, and the time of occurrence between beats of S1 and S2 acquired during different phases of the respiration cycle. The common dynamics in most subjects was attenuation of S1 during inspiration, accompanied by a small temporal delay, and accentuation of S2 during late inspiration and early expiration, with earlier occurrence of the aortic component and wider split morphology. Intensity changes induced to the heart sounds by the respiration cycle have been described by Ishikawa and Tamura, who compared heartbeats occurring in proximity to peak inspiration and peak expiration (15). They reported an increased intensity of both S1 and S2 during expiration. The results of the present study are consistent with these previous findings and provide a more extensive and precise analysis of the relations between heart sounds and respiration, owing to the utilization of computerized signal analysis. For some of the

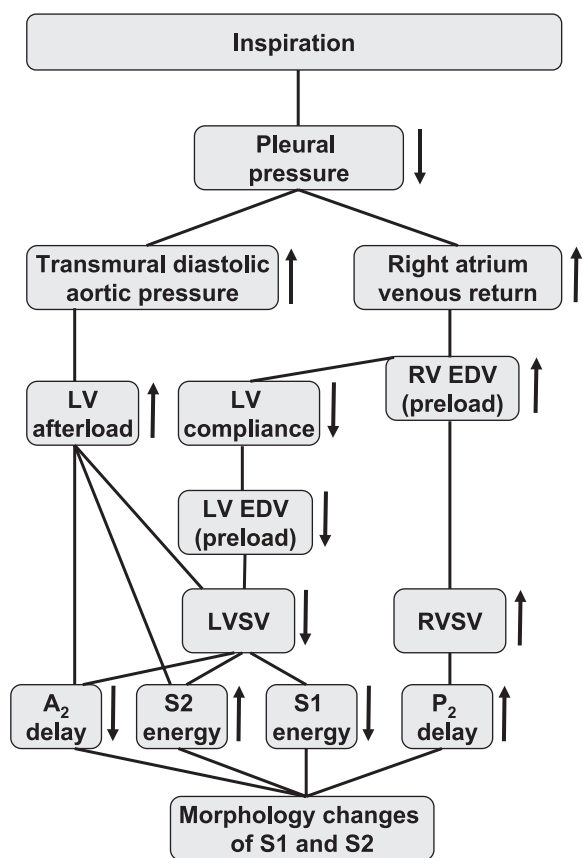


Fig. 9. Physiological factors affecting the morphology of heart sounds. During inspiration, there is an increase in the end-diastolic volume (EDV), or preload, of the right ventricle (RV) and a decrease in the preload of the left ventricle (LV). The latter causes a reduced contraction of the LV and attenuated S1. In addition, the increase in the LV afterload results in an earlier and accentuated aortic component of S2 ( $A_2$ ). The delay in the pulmonary component of S2 ( $P_2$ ) due to the larger and stronger RV stroke volume (SV) contributes to the split morphology of S2.

studied subjects, only a few of these respiration-induced changes were observed, and there was a large intersubject variability in the exact characteristics of the heart sound changes. We did not identify specific clinical characteristics that could explain this variability in a post hoc evaluation. In addition, as the group of subjects was relatively small, it was impractical to analyze the differences between subgroups.

The hemodynamic changes induced by inspiration to the atrial and arterial pressures are exaggerated during loaded inspiration (25, 26). We have used a simple experimental model of variable breathing resistances to obtain higher fluctuations of pleural pressure. In most of the studied subjects, respiration-induced changes in the timing and morphology of S1 and S2 were indeed more prominent in high-resistance respiration. As the amplitude of heart sounds was measured in uncalibrated units and was sensitive to slight movements of the transducers or the subjects, comparison of absolute energy content in different recordings was unreliable.

A new physiological insight from our current analysis is the relation between the breathing resistance and the relative temporal occurrence of the morphological changes in the respiratory cycle: with higher resistance, the heart sounds change earlier in inspiration. This is consistent with the hypothesis that

the lowered pleural pressure induces the sound changes, since, in high-breathing effort, the pleural pressure becomes low enough to affect the cardiovascular hemodynamics earlier in the respiratory cycle.

Automatic classification of respiratory phase and resistance level from the cluster-distance representation of S1 morphology achieved good average accuracy of  $87 \pm 7$  and  $82 \pm 7\%$ , respectively. These results provide additional credence to the relation between the respiratory condition and the heart sounds.

Classification of heart sounds has been studied before for identifying abnormalities of the heart valves, with good reported accuracy. The features used for classification were either specific spectral and morphological characteristics of the signal (10), or automatically selected features extracted by the wavelet transform (5, 24). The present study differs from this earlier work in both the technique and the application of the classification procedure. The method of representing the signal's morphology in the feature space of cluster distances provides a compact, automatically extracted feature set, which, unlike wavelet-based features, preserves the relation with the physiological meaning of the signal, and can therefore be more easily interpreted. This method enabled us to address a multi-class classification problem, and to apply it to prediction of respiratory-related variables, an entirely new applicative field of heart sound classification.

The classification performance achieved using S2 signals was inferior compared with S1, although the statistical analysis showed that S2 is undergoing morphological changes during respiration. A possible reason is that S2 has shorter duration and lower amplitude than S1, and its morphological changes are more subtle. In addition, the multicycle alignment of S2 signals is less accurate, as it is done without external ECG reference. Time-frequency representation by S-transform was chosen for S2 signals, as it was shown to be more robust to temporal misalignments and to provide better classification results than time-domain representation (2). Nevertheless, S2-based analysis remains more sensitive to noise interferences and signal misalignment and may require finer methods of signal alignment and distance measure to achieve more accurate clustering. The utilization of ECG for cycle segmentation and temporal location of S1 was a simplifying choice, which can be avoided by incorporating advanced methods of heart sound segmentation (13) into the analysis framework. Another limitation of the study concerns the complex relationship between the physiological processes producing the heart sounds and the morphology of the externally acquired acoustic signals. Factors other than cardiopulmonary interactions may affect the morphology of the acquired signals. These include the filtering effects of the thoracic cavity and the skin conducting the acoustic vibrations (11), as well as distortions by body movements, environmental noise, and noncardiac physiological sounds. While nonperiodic external noise is handled by the robustness of the clustering algorithm, which identifies and excludes irregular signal morphologies, the filtering effects of the thorax, lungs, and skin cannot be easily distinguished from the cardiopulmonary-induced modulation of the signals. However, the fact that opposite effects were consistently observed for S1 and S2 during inspiration (S1 was attenuated and delayed, while S2 was accentuated and occurred earlier) indicates that the contribution of the conducting medium is not a major determinant in the detected morphological changes of

the signals. To isolate the effects of the conducting medium, intrathoracic or transesophageal heart sound signals should be acquired as well, which naturally requires a much more invasive research protocol.

Quantitative analysis of heart sounds provided an unconventional tool for studying the complex cardiopulmonary mechanical interplay. The proposed framework for morphological analysis of acoustic heart signals can be further used for characterizing heart sounds alternations in clinical conditions of respiratory dysfunctions. Such conditions may include pulmonary congestion in heart failure patients, chronic obstructive pulmonary disease, asthma, and mechanical ventilation. Understanding the relations between heart sounds and cardiopulmonary mechanics may set the ground for a new technology of noninvasive, continuous patient monitoring.

#### REFERENCES

- Ahdesmaki M, Lahdesmaki H, Gracey A, Shmulevich L, Yli-Harja O. Robust regression for periodicity detection in non-uniformly sampled time-course gene expression data. *BMC Bioinformatics* 8: 233, 2007.
- Amit G, Gavriely N, Intrator N. Cluster analysis and classification of heart sounds. *Biomed Signal Process Control* 4: 26–36, 2009.
- Amit G, Gavriely N, Lessick J, Intrator N. Acoustic indices of cardiac functionality. In: *International Conference on Bio-inspired Systems and Signal Processing (BIO SIGNALS)*. Setubal, Portugal: INSTICC, 2008, p. 77–83.
- Benjamini Y, Hochberg Y. Controlling the false discovery rate: a practical and powerful approach to multiple testing. *J R Stat Soc Ser B* 57: 289–300, 1995.
- Bentley PM, Grant PM, McDonnell JT. Time-frequency and time-scale techniques for the classification of native and bioprosthetic heart valve sounds. *IEEE Trans Biomed Eng* 45: 125–128, 1998.
- Bernardi L, Porta C, Gabutti A, Spicuzza L, Sleight P. Modulatory effects of respiration. *Auton Neurosci* 90: 47–56, 2001.
- Bromberger-Barnea B. Mechanical effects of inspiration on heart functions: a review. *Fed Proc* 40: 2172–2177, 1981.
- Chen D, Durand LG, Lee HC, Wieting DW. Time-frequency analysis of the first heart sound. 3. Application to dogs with varying cardiac contractility and to patients with mitral mechanical prosthetic heart valves. *Med Biol Eng Comput* 35: 455–461, 1997.
- Chen D, Pibarot P, Honos G, Durand LG. Estimation of pulmonary artery pressure by spectral analysis of the second heart sound. *Am J Cardiol* 78: 785–789, 1996.
- Durand LG, Blanchard M, Cloutier G, Sabbah HN, Stein PD. Comparison of pattern recognition methods for computer-assisted classification of spectra of heart sounds in patients with a porcine bioprosthetic valve implanted in the mitral position. *IEEE Trans Biomed Eng* 37: 1121–1129, 1990.
- Durand LG, Langlois YE, Lanthier T, Chiarella R, Coppens P, Carioto S, Bertrand-Bradley S. Spectral analysis and acoustic transmission of mitral and aortic valve closure sounds in dogs. 1. Modelling the heart/thorax acoustic system. *Med Biol Eng Comput* 28: 269–277, 1990.
- Fisher R. Tests of significance in harmonic analysis. *Proc R Soc Lond* 125: 54–59, 1929.
- Gill D, Gavriely N, Intrator N. Detection and identification of heart sounds using homomorphic envelopegram and self-organizing probabilistic model. In: *Computers in Cardiology*. Piscataway, NJ: IEEE, 2005, p. 957–960.
- Heintzen P. The genesis of the normally split first heart sound. *Am Heart J* 62: 332–343, 1961.
- Ishikawa K, Tamura T. Study of respiratory influence on the intensity of heart sound in normal subjects. *Angiology* 30: 750–755, 1979.
- Knowles GK, Clark TJ. Pulsus paradoxus as a valuable sign indicating severity of asthma. *Lancet* 2: 1356–1359, 1973.
- Kusukawa R, Bruce DW, Sakamoto T, MacCanon DM, Luisada AA. Hemodynamic determinants of the amplitude of the second heart sound. *J Appl Physiol* 21: 938–946, 1966.
- Luisada AA, Portaluppi F. The main heart sounds as vibrations of the cardiohemetic system: old controversy and new facts. *Am J Cardiol* 52: 1133–1136, 1983.
- Nagendran T. The syndrome of heart failure. *Hosp Physician* 37: 46–57, 2001.
- Pinsky MR. Cardiovascular issues in respiratory care. *Chest* 128: 592–597, 2005.
- Rosner SW, Rodbard S. Beat-to-beat variation in the split second heart sound. *Am J Cardiol* 13: 333–339, 1964.
- Rushmer RF. *Cardiovascular Dynamics*. Philadelphia: Saunders, 1978.
- Sakamoto T, Kusukawa R, Maccanon DM, Luisada AA. Hemodynamic determinants of the amplitude of the first heart sound. *Circ Res* 16: 45–57, 1965.
- Say O, Dokur Z, Olmez T. Classification of heart sounds by using wavelet transform. In: *Proceedings of the Second Joint EMBS-BMES Conference, Houston, TX*. Piscataway, NJ: IEEE, 2002, p. 128–129.
- Scharf SM, Brown R, Saunders N, Green LH. Effects of normal and loaded spontaneous inspiration on cardiovascular function. *J Appl Physiol* 47: 582–590, 1979.
- Scharf SM, Graver LM, Khilnani S, Balaban K. Respiratory phasic effects of inspiratory loading on left ventricular hemodynamics in vagotomized dogs. *J Appl Physiol* 73: 995–1003, 1992.
- Shaver JA, Salerni R, Reddy PS. Normal and abnormal heart sounds in cardiac diagnosis. I. Systolic sounds. *Curr Probl Cardiol* 10: 1–68, 1985.
- Stockwell RG, Mansinha L, Lowe RP. Localization of the complex spectrum: the S-transform. *IEEE Trans Signal Process* 44: 998–1001, 1996.
- Van Leeuwen P, Kuemmel HC. Respiratory modulation of cardiac time intervals. *Br Heart J* 58: 129–135, 1987.